Direct observation of a dispersionless impurity band in hydrogenated graphene

D. Haberer,[1] L. Petaccia,[2] M. Farjam,[3] S. Taioli,[4,5] S. A. Jafari,[3,6] A. Nefedov,[7] W. Zhang,[7,8] L. Calliari,[4] G. Scarduelli,[4] B. Dora,[9] D. V. Vyalikh,[10] T. Pichler,[11] Ch. Wöll,[7] D. Alfè,[12,13,14] S. Simonucci,[15] M. S. Dresselhaus,[16] M. Knupfer,[1] B. Büchner,[1] and A. Grüneis[1,11]

[1]*IFW Dresden, P.O. Box 270116, D-01171 Dresden, Germany*

[2]*Elettra Synchrotron Light Laboratory, Sincrotrone Trieste SCpA, S.S. 14 Km 163.5, 34149 Trieste, Italy*

[3]*School of Nano Science, Institute for Research in Fundamental Sciences (IPM), P.O. Box 19395-5531, Tehran, Iran*

[4]*Interdisciplinary Laboratory for Computational Science (LISC), FBK-CMM and University of Trento, Via Sommarive 18, I-38123 Trento, Italy*

[5]*Department of Physics, University of Trento, Via Sommarive 14, I-38100 Trento, Italy*

[6] *Department of Physics, Sharif University of Technology, Tehran 11155-9161, Iran*

[7]*Institut für Funktionelle Grenzflächen (IFG), Karlsruher Institut für Technologie (KIT), Hermann-von-Helmholtz-Platz 1, D-76344 Eggenstein-Leopoldshafen, Germany*

[8]*National Synchrotron Radiation Laboratory, University of Science and Technology of China, 230029 Hefei, Anhui, People's Republic of China*

[9]*Department of Physics, Budapest University of Technology and Economics, Budafoki t 8, H-1111 Budapest, Hungary*

[10]*Institut für Festkörperphysik, TU Dresden, Mommsenstrasse 13, D-01069 Dresden, Germany*

[11]*Faculty of Physics, University of Vienna, Strudlhofgasse 4, A-1090 Wien, Austria*

[12]*Department of Earth Sciences, University College London, Gower Street, London WC1E 6BT, UK*

[13]*Department of Physics and Astronomy, University College London, Gower Street, London WC1E 6BT, UK*

[14]*London Centre for Nanotechnology, University College London, Gower Street, London WC1E 6BT, UK*

[15]*Department of Physics, University of Camerino, Via Madonna delle Carceri 9, I-62032 Camerino, Italy*

[16]*Department of Physics and Department of Electrical Engineering and Computer Science, Massachusetts Institute of Technology, Cambridge, MA 02139-4307, USA*

(Received 21 October 2010; revised manuscript received 22 February 2011; published 22 April 2011)

We show with angle-resolved photoemission spectroscopy that a new energy band appears in the electronic structure of electron-doped hydrogenated monolayer graphene (H-graphene). Its occupation can be controlled with the hydrogen amount and allows for tuning of graphene's doping level. Our calculations of the electronic structure of H-graphene suggest that this state is largely composed of hydrogen 1*s* orbitals and remains extended for low H coverages despite the random chemisorption of H. Further evidence for the existence of a hydrogen state is provided by x-ray absorption studies of undoped H-graphene which are clearly showing the emergence of an additional state in the vicinity of the π^* resonance.

DOI: 10.1103/PhysRevB.83.165433 PACS number(s): 73.22.Pr, 61.72.−y, 79.60.−i

I. INTRODUCTION

Doping is at the heart of modern semiconductor technology because it allows for control of the carrier density and is therefore the basis for all circuit elements. If the concentration of the dopant increases beyond a critical value, the physical properties of a doped semiconductor are described by impurity band formation.[1] For example in the case of B-doped diamond an insulator-to-metal transition and superconductivity is observed beyond a critical B concentration.[2] From angle-resolved photoemission spectroscopy (ARPES)[3] and x-ray absorption spectroscopy[4] of B-doped diamond, it was concluded that the impurity band derived from B orbitals is above E_F. Covalent doping is also successfully applied to sp^2 bonded carbon materials.[5] It has been shown that hydrogen readily forms a covalent bond with graphene.[6] The bonding environment of C-H is usually well defined and H/C ratios equal to ∼25% have been realized.[7,8] It is therefore tempting to ask whether impurity band formation happens in hydrogenated graphene (H-graphene), in close analogy to B-doped diamond. Theory suggests H-graphene[9] to have a substantial band gap of 1 eV accompanied by a dispersionless and spin-polarized midgap state.[10–12] Transport experiments have shown that the exposure of graphene to atomic hydrogen turns graphene into an insulator with a temperature dependence of the conductivity that points toward a variable range hopping mechanism.[13] For electron-doped (*n*-doped) graphene on SiC, small H amounts yield a shrinkage of the Fermi surface, and a metal-to-insulator transition (MIT) has been observed with a combined transport and ARPES study.[14] For pristine quasi-free-standing graphene, the opening of a band gap has been reported upon hydrogenation.[7,15] However, the formation of a hydrogen impurity band has not yet been observed experimentally and therefore the question of its existence and electronic properties remains an open topic.

In this work we present the first experimental evidence of a hydrogen-derived midgap state in H-graphene using ARPES and near-edge x-ray absorption fine structure (NEXAFS) measurements. The latter method provides access to unoccupied electronic states above the Fermi level by measuring the x-ray absorption which is caused by transitions from the C 1*s* core level to the π^* and σ^* energy bands. For undoped H-graphene the impurity band is located within the emerging gap at the Fermi level and is therefore hardly accessible with ARPES since this method probes only the occupied electronic states

of the band structure. Using potassium intercalated n-doped graphene, the hydrogen-derived state becomes available for an occupation with electrons and acts as an acceptor level for π^* electrons which can be directly observed in ARPES.

Density functional theory (DFT) calculations suggest that the midgap state is largely derived from H 1s orbitals. Calculations of the typical and average density of states (DOS) using the kernel polynomial method (KPM) with a tight-binding (TB) band structure calculation[11,16] indicate that the new state does not localize easily despite the randomness in the H chemisorption sites.

II. EXPERIMENTAL METHODS

Pristine monolayer graphene samples were prepared *in situ* under ultrahigh vacuum conditions by chemical vapor deposition on Ni(111) thin films epitaxial grown on W(110).[17] Then one monolayer (ML) of Au was deposited on graphene and intercalated into the graphene/Ni interface by annealing.[7,18,19] This procedure liberates graphene from the strong interaction to the Ni substrate, rendering it quasi–free standing. Functionalization was performed by exposing pristine graphene to potassium atoms which were evaporated from commercial SAES metal dispensers while the graphene sample was kept at 25 K during the deposition. Potassium intercalation into the graphene/Au interface was performed at room temperature (RT). Hydrogenation was carried out at $\sim 1\times10^{-9}$ mbar for times between 1 and 100 s. The atomic hydrogen beam was produced by cracking H_2 at 3000 K in a tungsten capillary. ARPES measurements were carried out at the BaDElPh beamline of the Elettra synchrotron in Trieste (Italy).[20] The spectra were acquired at photon energies of 26 eV and 40 eV with the sample at 25 K and a base pressure better than 8×10^{-11} mbar. The angular resolution was 0.15° and the energy resolution was set to 15 meV. All ARPES measurements were taken along the $\Gamma K M$ directions. Furthermore, we performed NEXAFS measurements at the carbon K edge using synchrotron radiation. These studies were carried out at BESSY II using the HESGM beamline equipped with a home-built channeltron detector. The NEXAFS spectra were measured in the partial electron yield mode. We have applied a negative retarding potential of $U = -150$ V.

III. RESULTS AND DISCUSSION

We discuss the electronic properties of hydrogenated graphene intercalated with Au using NEXAFS. As this method probes the unoccupied density of states by inducing dipole transitions from the C 1s core levels to the π^* energy band, it is a versatile technique to investigate the changes in the electronic structure that appear upon hydrogenation. In Figs. 1(a) and 1(b) we show the NEXAFS spectra for pristine and H-graphene (H/C $\sim$ 15%),[7] respectively. Both sets of curves depict a similar behavior with ϕ, the angle of light incidence: For grazing incidence ($\phi = 20°$) we have a maximum photoabsorption referring to the π^* resonance and for normal incidence ($\phi = 90°$) we have a maximum absorption identified as the σ^* resonance. This is in agreement with the NEXAFS experiments performed on graphite and previous measurements on graphene.[7,21,22] A closer look at

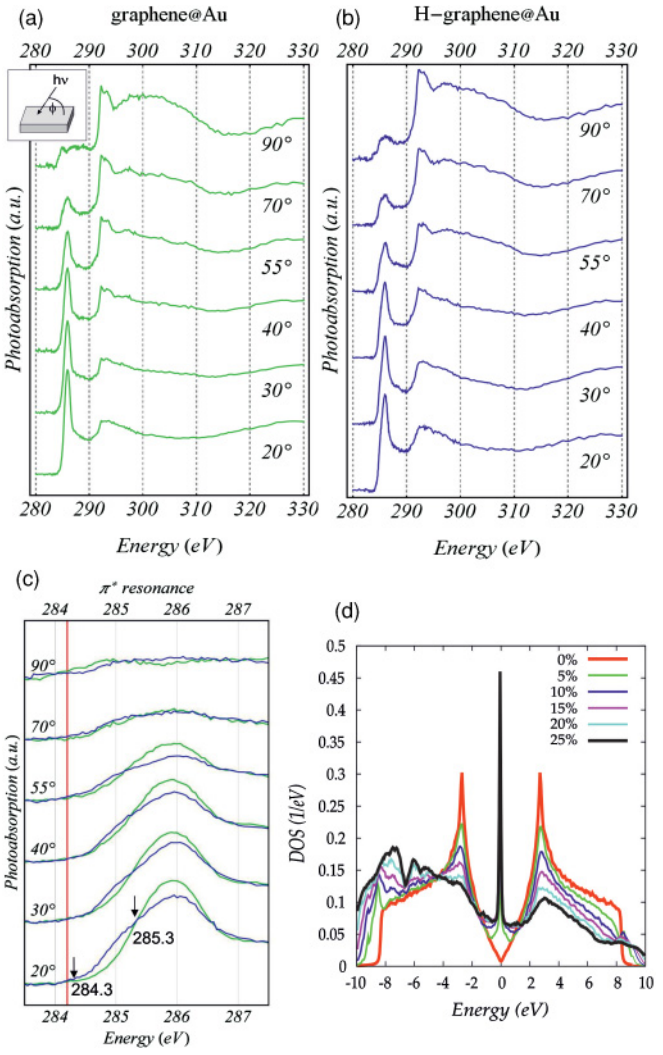

FIG. 1. (Color online) NEXAFS spectra of (a) pristine graphene and (b) hydrogenated graphene (H/C $\sim$ 15%) for various incident angles between normal (90°) and grazing incidence (20°). The inset in (a) shows the experimental geometry and ϕ, the angle of light incidence. (c) Comparison of pristine (green) and H-graphene (blue) in the region of the π^* resonance. The additional shoulder at lower photon energy denoted by two arrows is best visible for grazing incidence. The red line indicates the C 1s energy position of unhydrogenated graphene/Au. (d) Calculated density of states for hydrogenated graphene with various H/C ratios.

the π^* resonance is shown in Fig. 1(c). Two observations can be made from the comparison of pristine and H-graphene: (1) the π^* resonance gets weaker in intensity upon hydrogenation and (2) the high-resolution spectra show a low-energy shoulder appearing upon hydrogenation for grazing incidence. Observation 1 can be well understood since hydrogen adsorption effectively removes π bonds (sp^3 C-H bond). Concerning observation 2, the feature appears between 284.3 eV and 285.3 eV, as indicated by the arrows in Fig. 1(c). In the following we argue that this extra feature can also be attributed to a midgap state that lies in between the π and π^* bands. Such a feature can contribute to a downshift of the π^* resonance. To 0th order the NEXAFS resembles the unoccupied density of states (neglecting the light polarization, excitonic, and

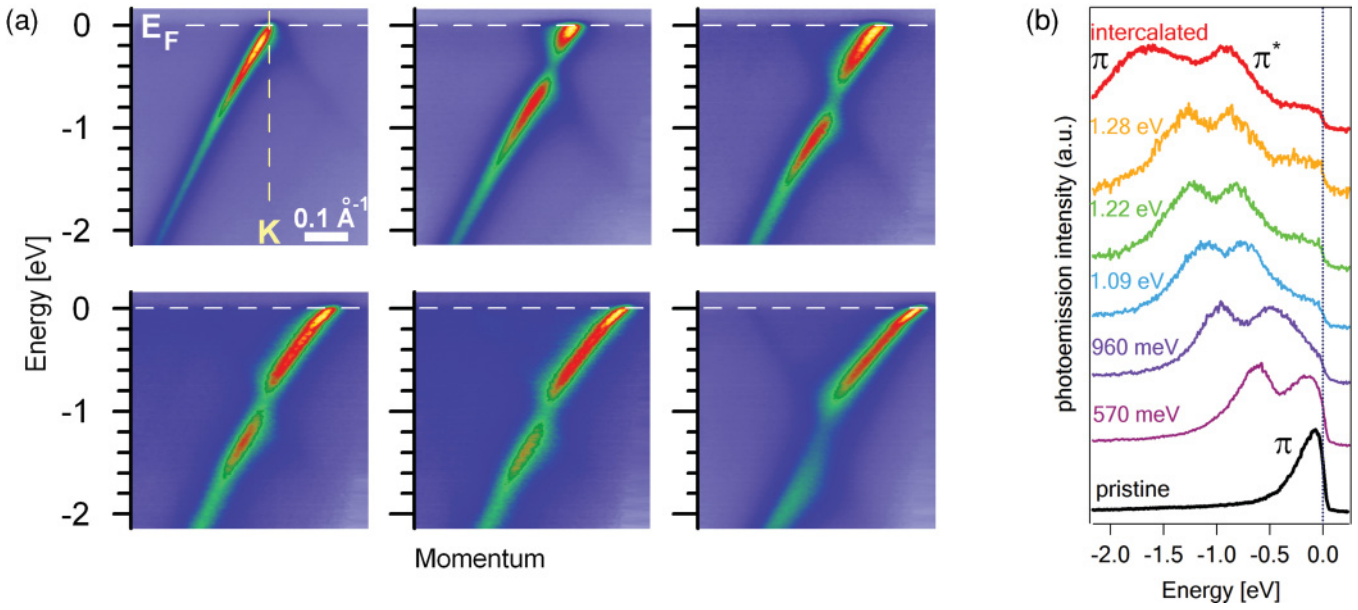

FIG. 2. (Color online) (a) ARPES intensities around the K point of the Brillouin zone of graphene intercalated with one monolayer Au for increasing potassium doping. The last viewgraph (bottom right) denotes the photoemission intensities of graphene intercalated with potassium in between the graphene/Au interface. (b) Energy dispersion curves taken at the K point for the six doping steps in (a) with the shift of E_F as indicated. For the doped graphene, the two peaks correspond to the π and π^* bands. Upon intercalation of potassium between graphene and Au, the value of the gap between π and π^* bands doubles.

matrix element effects). A comparison with the calculated DOS is therefore key to assign the measured feature at the π^* resonance to an electronic state. To that end we performed tight-binding (TB) calculations of the DOS of disordered H-graphene using the equation-of-motion method for various values of H coverages.[23] This method allows us to treat large systems with adjustable hydrogen coverages. In this case we chose graphene with 180 000 C atoms for the calculations. The TB parameters we used were $\gamma = -2.7$ eV for the C-C interaction energy, $\gamma_i = -5.7$ eV for the C-H hopping energy, and $\epsilon_i = -0.2$ eV for the on-site energy of the hydrogen orbital.[23] In Fig. 1(d) we depict the calculated density of states of C_nH for various C/H ratios in agreement with previous calculations of disordered graphene.[23] It can be seen that with increasing H/C ratio, a new electronic state appears in between the π and π^* bands at the Fermi energy. Looking at Fig. 1(c) the additional shoulder at the π^* resonance also appears close to the onset (the edge of the conduction band in Fig. 1 is located at 284.2 eV). It is therefore likely that the additional shoulder in NEXAFS is a fingerprint of a hydrogen-derived midgap state. Such midgap states have been theoretically predicted[10] but have not been observed so far in graphene. Their existence may have implications for superconductivity comparable to the case of boron-doped diamond[2–4] as well as magnetism and optical properties of H-graphene.[10] The spectral contribution of these new states can be engineered for attainable H/C ratios by exposing graphene to an H beam for a defined time. However, it should be noted that the observed shoulder in the vicinity of the π^* resonance cannot exclusively be attributed to a hydrogen midgap state as it is also possible that changes in the carbon bond configurations at the hydrogenation sites contribute to the observed shoulder in NEXAFS.[22]

Therefore, we turn to an alternative strategy which comprises the doping of graphene with additional electrons. This results in a shift of the Fermi level with respect to the Dirac point so that the hydrogen midgap state becomes populated with electrons and should be observable with ARPES. A well-known approach from graphite is the intercalation of potassium,[24,25] since alkali metals donate their electrons without forming covalent bonds which might influence the hydrogenation procedure. Figure 2(a) shows ARPES spectra of monolayer graphene with an increasing potassium coverage. The first viewgraph (upper left) in Fig. 2(a) corresponds to undoped graphene and one can see the π band touching E_F at the K point in the Brillouin zone. Clearly, the Dirac point shifts away from E_F to higher energies with increasing potassium coverage up to a final value of $\sim$1 eV. It has been put forward that the small gap in the spectral function at the K point originates from the Au superstructure which breaks the AB symmetry.[26] Warming up the sample to RT and cooling to 25 K again yields a completely different picture shown in the last panel (bottom right) of Fig. 2(a): A much larger separation between π and π^* at the K point is observed. We attribute this to the intercalation of potassium atoms into the graphene/Au interface, consistent with the behavior of other metals (Au, Ag, Fe, Cu...) that readily intercalate in between the interface of graphene and the Ni substrate.[7,19,27,28] The intercalation at RT is also consistent with the reported 100 K temperature limit above which potassium ions on a graphene sheet become mobile.[29] Upon potassium intercalation the gap between the π and π^* bands increases which could be explained by the fact that the Au lattice forces the potassium ions to positions which distort the graphene lattice and further break the AB symmetry of the carbon atoms. The energy dispersion

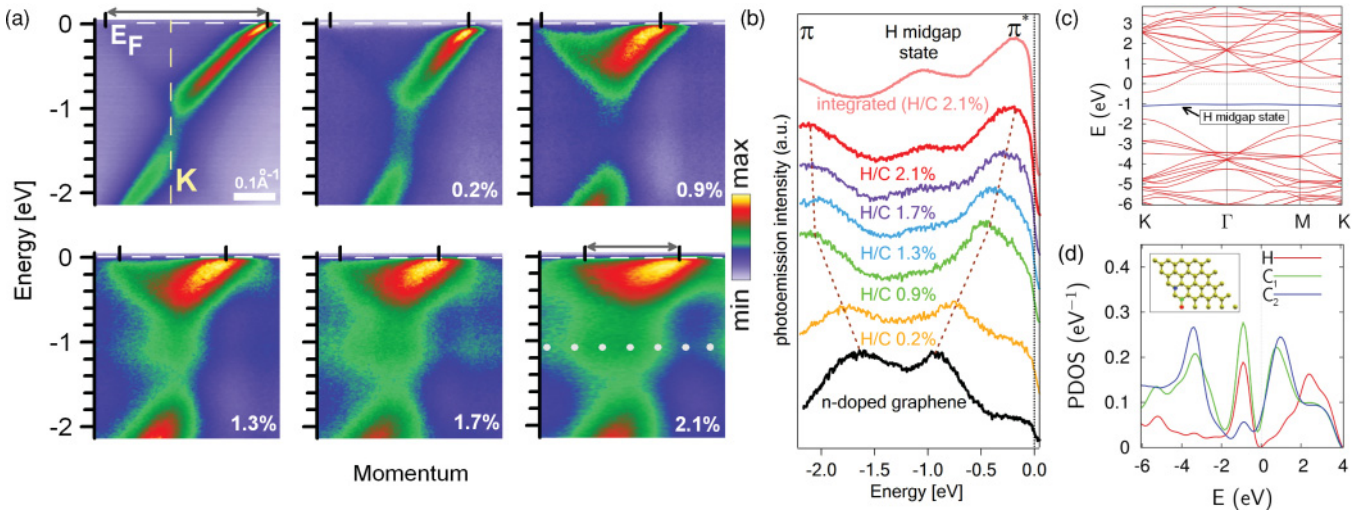

FIG. 3. (Color online) (a) ARPES intensities around the K point of the Brillouin zone of hydrogenated n-doped graphene with increasing H/C ratios as denoted in percent. The size of the Fermi surfaces is indicated by two black vertical ticks on top and an arrow for the H/C = 0 and H/C = 2.1% ratios. The dots in the last panel are a guide to the eye and depict the dispersionless midgap state. The photoemission intensity scale is depicted and applies to all graphs. (b) Energy dispersion curves of the ARPES intensity at the K point. (c) DFT calculation of the electronic energy bands and (d) the partial DOS of HC_{32}. A rigid band shift of 1 eV was applied in (c) to account for the potassium doping. The dispersionless band 1 eV below E_F in blue corresponds to the midgap state. The inset to (d) depicts the unit cell and the atoms (H, C_1, and C_2) in the graphene lattice which contribute significantly to the midgap-state DOS.

curves (EDCs) at the K point are shown in Fig. 2(b) for the potassium-doping steps. The n doping does not significantly change the separation between the π and π^* bands. However, upon potassium intercalation the energy separation increases from 400 meV to 800 meV. We purposefully induce this "gap" for a direct observation of the hydrogen acceptor level which we will discuss below.

In Fig. 3(a) we present ARPES spectra of a hydrogenation series that was performed on fully n-doped graphene. In the potassium intercalated graphene with the larger gap between π and π^*, the graphene layer provides a buffer between potassium ions and H atoms on top of graphene which efficiently prevents chemical bonding.[30] From the hydrogenation series in Fig. 3(a) we observe (i) a general broadening of the spectra, (ii) a shrinkage of the Fermi surface pointing towards hole doping, (iii) that the gap between π and π^* increases with hydrogenation, and most importantly, (iv) that a new state appears within this gap. The new state is almost dispersionless and its ARPES intensity increases as hydrogenation proceeds. The increased ARPES intensity of the midgap state and the shrinkage of the Fermi surface of the π^* band as indicated by the two black vertical ticks on top of each panel in Fig. 3(a) go together and are attributed to an electron transfer from the π^* band to the midgap state. We employ the Fermi surface shrinkage to calculate the H/C ratio[14] which is depicted for each hydrogenation step in Figs. 3(a) and 3(b). Notably, this estimation of the H/C ratio is based on the assumption that each hydrogen atom accepts one electron.[14] Hence a smaller charge transfer to the acceptor hydrogen level would lead to effectively higher H/C ratios. As we will show later, the acceptor level forms an impurity band which does not localize for the low H/C ratios (∼1%) shown here, despite the randomness in H positions.

In Fig. 3(b) we depict an analysis of the spectral functions from Fig. 3(a) of hydrogenated n-doped graphene at the K point which fortifies our findings. Already at ratios of H/C $= 0.9\%$ the energetic distance between the π and π^* bands increases from 0.8 eV to 1.6 eV which we attribute to the partial sp^3 hybridization as discussed previously.[7] The EDCs integrated over all k values for H/C $= 2.1\%$ [from last panel of Fig. 3(a)] unambiguously visualizes the new electronic state between 0.7 eV and 1.6 eV [top curve of Fig. 3(b)]. The lack of a dispersion of this feature can be clearly seen when comparing the integrated EDC with the single EDC taken at the K point. Whereas the shape of the midgap state is nearly identical in both curves, only the intensity of this state is increased when integrating the EDCs in k space. Figure 3(c) shows DFT calculations of the band structure of H-graphene HC_{32} in agreement with previous calculations,[10] which is comparable to that measured for the highest H/C ratio of 2.1%. To account for the n doping from potassium atoms, we applied a rigid shift by 1 eV. Clearly, there is an almost dispersionless shallow acceptor level also present in the calculation which we identify as the new electronic midgap state at ~ -1 eV that we have found using ARPES. For a complete understanding of the origin of this new state, we project the DOS on the C $2p_z$ and H $1s$ orbitals. We consider C $2p_z$ from the hydrogenated site up to the third-nearest neighbor. Figure 3(d) depicts the projected DOS for the midgap state. Interestingly, the contribution of the $2p_z$ orbital of the same sublattice of the hydrogenated C atom is almost zero. From the projected DOS it is evident that the midgap state is made up largely from H $1s$ orbitals and the C $2p_z$ orbitals from the neighboring lattice site. In Fig. 3(d) these two atoms are indicated by H and C_1. The supplementary figure S4 depicts a realistic DFT calculation of hydrogenated graphene on a K/Au substrate and indicates that the midgap state is robust against substrate interactions.[31]

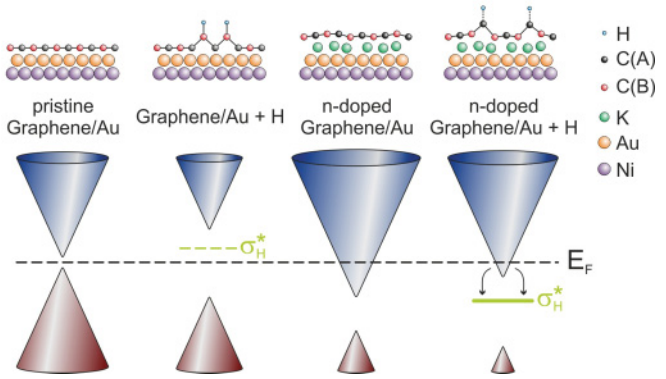

FIG. 4. (Color online) Sketches of symmetry-breaking, hybridization, and charge-transfer processes in pristine and n-doped H-graphene. In the case of undoped hydrogenated graphene the hydrogen-derived midgap state can be measured with absorption spectroscopies probing unoccupied states such as NEXAFS. Only if E_F is above the energetic position of the midgap state (denoted by σ_H^*) can it be directly observed in ARPES. In this case, the midgap state likely accepts electrons from the π^* band of graphene denoted by arrows (see the right panel).

Our present data suggest that the midgap state always exists in hydrogenated graphene, but its position with respect to E_F determines whether it is observable by ARPES which probes only occupied states or absorption spectroscopies such as NEXAFS measuring unoccupied states above the Fermi level. A sketch of the ongoing symmetry-breaking, charge-transfer, and hybridization processes in pristine and n-doped H-graphene is shown in Fig. 4.

Finally, we investigate impurity band formation and electron localization in H-graphene which governs its transport and optical properties. On the one hand, a minimum concentration (Mott criterion) is needed for band formation, but on the other hand, too much disorder can induce electron localization in both the π electron bands and the midgap state. A very low H impurity concentration leads to midgap energy levels corresponding to bound states. The radius of such bound states is given by $a_B = e^2/(2\epsilon E_B)$ where ϵ is the relative dielectric constant of the host material (in this case graphene) and E_B is the binding energy of the acceptor level. The Mott criterion[1] for the formation of a metallic band from such discrete levels states that the concentration n_c of the impurities must be high enough to satisfy $n_c^{1/2} a_B \approx 1/4$. Assuming the H/C ratio to be η, the critical concentration will be given by $\eta_c = 0.007(\epsilon E_B)^2$. In our case the position of the impurity band with respect to E_F is given by $E_B \approx -1.0$ eV, and with $\epsilon \approx 2$ the critical concentration needed for metallization is $\eta_c \sim 1.4\%$. Therefore when the concentration of H atoms is $\sim 1\%$, we expect the formation of an impurity band. However, since the position of H adsorbates is random (see supplementary information), the question of the localization of impurity band states arises. To answer this question, we use the KPM method to calculate the typical electron density of states, wherein the vanishing of this DOS indicates localization.[16] In Fig. 5 we have depicted the average DOS and the typical DOS for H-graphene within a TB model.[11] Such a TB model, although ignoring the effect

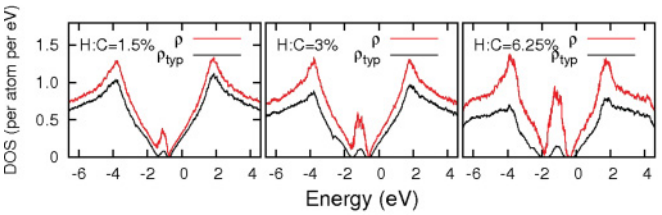

FIG. 5. (Color online) The calculated typical (black line) and average (red line) DOS for three different H/C ratios. The vanishing of the typical DOS at energies slightly higher or lower than the acceptor level (located at $E = -1$ eV) indicates a localization of the π-band edges. The typical DOS of the midgap state never reaches zero which indicates that it is resistant to localization. A relatively large width of the impurity band helps the states in the middle of the impurity band remain extended.

of the substrate, is consistent with our ARPES data for the nonhydrogenated samples which show perfect Dirac cone dispersion. When the concentration of H atoms is very low, the model results in an effective Hamiltonian for C atoms only, with an energy-dependent on-site potential.[11] However, when the H impurity concentration is comparable to η_c, in addition to the energy-dependent random potential (Anderson type), the hydrogenic wave functions will have substantial overlap to give rise to an impurity band. Moreover, for moderate values of the diagonal on-site disorder $W \approx \gamma$, where W is the range of the on-site energies and γ is the C-C hopping energy, a mobility edge emerges in the conduction and valence bands.[16] The acceptor band survives the randomness regarding the position of the H atoms, and the states in the center of the acceptor band remain extended and a localization of these states is not expected. As can be seen in Fig. 5, a vanishing of the typical DOS indicates that the states close to the edges of the impurity band get localized, but due to the substantial bandwidth, states in the middle of the band remain extended. Therefore, although the impurity band has no dispersion as indicated by the ARPES measurements of the spectral function, it nevertheless has a sufficiently large bandwidth, so as to provide enough kinetic energy to enable conduction within this band. For very low concentrations, a localization of charge carriers in this impurity state would be expected, as the right and left mobility edges of the impurity band are expected to merge when the impurity band becomes narrow enough.

IV. CONCLUSIONS

In conclusion, we have found a new electronic state in H-graphene that is located between the π and π^* bands. For undoped H-graphene this state is energetically situated within the gap around E_F and is accessible with absorption spectroscopies such as NEXAFS. In the case of n-doped H-graphene the midgap state becomes available for electrons and directly observable with ARPES since it is then situated below E_F. Therefore, the H impurity band likely acts as an electron acceptor level which provides the possibility to control the electron concentration in H-graphene via the H/C ratio. An estimation of the Mott criterion and a calculation of the typical DOS suggests that above H/C $\sim 1\%$ and below H/C $\sim 6\%$, the acceptor level can form an extended impurity band. DFT

calculations of the DOS show this new band to be largely composed from H 1*s* orbitals. Hence the new electronic state we found is expected to give rise to metallic conduction when the chemical potential is tuned to cross the impurity band. Furthermore the questions of a spin splitting of the impurity band and the magnetic properties of H-graphene arise as has been suggested by theoretical calculations.[10] Further studies including spin-resolved methods might be necessary to address these open questions and gain more detailed insights into the nature of this new electronic state in H-graphene.

ACKNOWLEDGMENTS

D.H. and A.G. acknowledge funding from the European Community's Seventh Framework Program (FP7/2007-2013) under Grant Agreement No. 226716 for their stay at the Elettra synchrotron. A.G. and G.S acknowledge funding from the European Community's Seventh Framework Programme (FP7/2007-2013) under grant agreement 226716 for their stay at the BESSY synchrotron. M.F. acknowledges funding from the Iranian Nanotechnology Initiative. S.A.J. acknowledges the National Elite Foundation (NEF) of Iran for financial support. S.A.J. was supported by the Vice Chancellor for Research Affairs of the Isfahan University of Technology (IUT). S.T. and S.S. acknowledge CINECA (Bologna, Italy) and HECToR consortia (UK) for providing access to high-performance supercomputers. S.T. acknowledges funding from the European Community's Seventh Frame Program (2007-2013) and the Autonomous Province of Trento under Call 4–researcher 2009–Outgoing COFUND. B.D. was supported by the Hungarian Scientific Research Fund No. K72613 and by the Bolyai program of the Hungarian Academy of Sciences. T.P. acknowledges Project No. FWF-I377-N16. D.V. acknowledges DFG Grant No. VY 64/1-1. A.N., W.Zh., and Ch. W. acknowledge funding from the NanoMikro Programme (Project No. 431103–Molecular Building Blocks/Supramolecular Networks). M.S.D. acknowledges support from NSF/DMR 10-04147. D.H., M.K., and A.G. acknowledge funding from DFG Project No. GR 3708/1-1. A.G. acknowledges an APART fellowship and an MC reintegration grant (ECO-graphene). We acknowledge M. Löffler for help in preparing this manuscript and D. Lonza, S. Leger, R. Hübel, and R. Schönfelder for technical assistance during the experiments.

[1] S. N. Mott, *Metal Insulator Transitions* (Taylor & Francis, London, 1991).
[2] E. A. Ekimov *et al.*, Nature (London) **428**, 542 (2004).
[3] T. Yokoya *et al.*, Nature (London) **438**, 647 (2005).
[4] J. Nakamura, N. Yamada, K. Kuroki, T. Oguchi, K. Okada, Y. Takano, M. Nagao, I. Sakaguchi, T. Takenouchi, H. Kawarada, R.C.C. Perera, and D.L. Ederer, J. Phys. Soc. Jpn. **77**, 054711 (2008).
[5] D. W. Boukhvalov and M. I. Katsnelson, J. Phys. Condens. Matter **21**, 344205 (2009).
[6] J. O. Sofo, A. S. Chaudhari, and G. D. Barber, Phys. Rev. B **75**, 153401 (2007).
[7] D. Haberer *et al.*, Nano Lett. **10**, 3360 (2010).
[8] A. Nikitin, L.-A. Näslund, Z. Zhang, and A. Nilsson, Surf. Sci. **602**, 2575 (2008).
[9] V. V. Cheianov, O. Syljuåsen, B. L. Altshuler, and V. Fal'ko, Phys. Rev. B **80**, 233409 (2009).
[10] E. J. Duplock, M. Scheffler, and P. J. D. Lindan, Phys. Rev. Lett. **92**, 225502 (2004).
[11] J. P. Robinson, H. Schomerus, L. Oroszlány, and V. I. Falko, Phys. Rev. Lett. **101**, 196803 (2008).
[12] S. Casolo, O. M. Lovvik, R. Martinazzo, and G. F. Tantardini, J. Chem. Phys. **130**, 054704 (2009).
[13] D. C. Elias *et al.*, Science **323**, 610 (2009).
[14] A. Bostwick J.L. McChesney, K.V. Emtsev, Th. Seyller, K. Horn, S.D. Kevan, and E. Rotenberg, Phys. Rev. Lett. **103**, 056404 (2009).
[15] R. Balog *et al.*, Nature Mater. **9**, 315 (2010).
[16] M. Amini, S. A. Jafari, and F. Shahbazi, Europhys. Lett. **87**, 37002 (2009).
[17] A. Grüneis, K. Kummer, and D. V. Vyalikh, New J. Phys. **11**, 073050 (2009).
[18] A. M. Shikin, G. V. Prudnikova, V. K. Adamchuk, F. Moresco, and K.-H. Rieder, Phys. Rev. B **62**, 13202 (2000).
[19] A. Varykhalov *et al.*, Phys. Rev. Lett. **101**, 157601 (2008).
[20] L. Petaccia *et al.*, Nucl. Instrum. Methods Phys. Res. A **606**, 780 (2009).
[21] J. Fink *et al.*, Solid State Commun. **47**, 687 (1983).
[22] M. L. Ng *et al.*, J. Phys. Chem. C **114**, 18559 (2010).
[23] S. Yuan, H. De Raedt, and M. I. Katsnelson, Phys. Rev. B **82**, 115448 (2010).
[24] M. S. Dresselhaus and G. Dresselhaus, Adv. Phys. **30**, 139 (1981).
[25] A. Grüneis *et al.*, Phys. Rev. B **80**, 075431 (2009).
[26] C. Enderlein, Y. S. Kim, A. Bostwick, E. Rotenberg, and K. Horn, New J. Phys. **12**, 033014 (2010).
[27] Y. S. Dedkov *et al.*, Phys. Rev. B **64**, 035405 (2001).
[28] Y. S. Dedkov, M. Fonin, U. Rüdiger, and C. Laubschat, Appl. Phys. Lett. **93**, 022509 (2008).
[29] J. Barnard, K. Hock, and R. Palmer, Surface Science **287**, 178 (1993).
[30] J. S. Bunch *et al.*, Nano Lett. **8**, 2458 (2008).
[31] See supplementary material at [http://link.aps.org/supplemental/10.1103/PhysRevB.83.165433] for a more comprehensive description of the calculations.